CHEMICAL ENGINEERING TRANSACTIONS
VOL. 92, 2022
A publication of AIDIC
The Italian Association of Chemical Engineering
Online at www.cetjournal.it
Guest Editors: Rubens Maciel Filho, Eliseo Ranzi, Leonardo Tognotti

ISBN 978-88-95608-90-7; **ISSN** 2283-9216
DOI: 10.3303/CET2292094

Adsorption of Nickel in a Continuous System using Biochar Obtained from Pyrolysis of Rice Husk at Low Temperature

Mario R. Alvear-Alayon, Liset P. Mallarino* , Luz M. Ramos, Carlos M. Arrieta, Jesus D. Guerra, Jalelys L. Leones, Lesly P. Tejeda

Biomedical, Toxicological, and Environmental Sciences Research Group (BIOTOXAM). Zaragocilla Campus. Faculty of Medicine, Universidad de Cartagena, Zaragocilla. Cra. 50 No. 29 - 11, Cartagena, Colombia.
lmallarinom@unicartagena.edu.co

This work evaluates the properties of the biochar obtained through the pyrolysis of rice husk at low temperature and its use as adsorbent of nickel in a continuous system. The particle size and the pyrolysis time of the biomass were varied. Yield, the percentage of carbon, functional groups, surface area and calorific value was determined. The yield of the biochar was obtained between 30.85 and 41.78%, obtaining the best results for the particle size of 0.5 mm and the pyrolysis time of 12 h, while the highest percentage of carbon was of 26. 66%, an adsorption column was designed for the removal of nickel from pollution water using biochar derived from rice husk as an adsorbent material for its subsequent scaling to pilot scale dimensions. For this study, experiments were performed in the built adsorption column, where water samples were taken at the exit of the commune every 15 minutes until arriving at 2 hours, for further analysis, calculation of removal percentages, construction of rupture curves and determination of scaling parameters of the column. Removal percentages between 19% and 86%, break times between 12 and 46 minutes were found, obtaining the best percentages with a height of 20 cm and 25 ppm of nickel. Unused bed heights that be determined were 12.11 cm and 7.23 cm. Finally, was analysed how was the development of the adsorption process in each case and the behaviour of the breakthrough curve biochar respect to activated carbon, which showed that this technology can be a moderately viable alternative since the functional groups and the high surface area activated carbon has make it better adsorbent biochar.

1. Introduction

The growth of rice generates approximately eight hundred and twenty-two million tons of waste annually around the world, of which more than 90% are burned outdoors or discharged into rivers and oceans to dispose of them. The rice husk represents approximately 20% of the total weight of the grain and its final disposal constitutes serious environmental problems (Dunnigan, et al., 2018).

Many thermochemical conversion technologies have been used for the reuse of biomass, among which are liquefaction, gasification and direct combustion, however, its application has been decanted for other types of waste such as sugar cane bagasse of sugar, fruit peels, corn straw, tuber shells and others (Noë, Billen, & Garnier, 2017). Pyrolysis in the last decade has developed as the most promising thermochemical method to produce energy from biomass. Recent investigations shows that both, the origin of the raw material and production conditions are important to determine the performance and properties of biochar. The chemical compounds of the raw material, with the pyrolysis temperature are the main factors that greatly affect the biochar and characteristics of its surface. The biochar obtained by pyrolysis from agroindustrial waste can be used as an adsorbent material for pesticides, heavy metals, aromatic hydrocarbons, as soil and fuel recovery. Pollution with heavy metals today has increased due to anthropogenic contributions, coming from mining, industrialization, rapid urbanization and the growing dependence on fossil fuels (Singh & Kumar, 2017). Among the heavy metals, one of the most relevant is the Nickel. Nickel-based super alloys have excellent mechanical properties and good corrosion resistance at high service temperatures are extensively used in aviation and aerospace industries. Recent studies have been developed for the removal of heavy metals in water bodies

Paper Received: 13 February 2022; Revised: 8 March 2022; Accepted: 27 April 2022
Please cite this article as: Alvear-Alayon M.R., Mallarino-Miranda L., Ramos L.M., Arrieta C.M., Guerra J.D., Leones J.L., Tejeda-Benitez L., 2022, Adsorption of Nickel in a Continuous System Using Biochar Obtained from Pyrolysis of Rice Husk at Low Temperature, Chemical Engineering Transactions, 92, 559-564 DOI:10.3303/CET2292094

using different adsorbents, such as biochar from olive solid waste (Abdelhadi, Dosoretz, Rytwo, & Gerchman, 2017), activated carbon (Popa & Visa, 2017), adsorbents based on dendritic polymers (Sajid, 2017), but some technologies that use commercial activated carbons, such as granular activated carbon (GAC), are expensive, so it has been necessary to look for other technologies more economic (Dalai, Jha, & Desai, 2015a). For this reason, biochar derived from rice husk is presented as a good alternative for removing nickel from polluted waters.

2. Materials and methods

2.1 Obtaining biochar

About 50 g of rice husk was washed with 200 mL of distilled water, then biomass was filtered and dried for 2 days outdoor, and then in an oven for 2 hours at 100°C. The rice husk was ground and sieved to obtain size particles of 0.212, 0.355, and 0.5 mm. The pyrolysis of 50 g of rice husk was conducted in vacuum furnace at a 200°C for 8 and 12 h. The yield of the biochar production was calculated as the quotient between the mass of biochar and the mass of biomass.

2.2 Characterization of the biochar

For measuring the percentage of carbon, thermogravimetry is used, a technique that offers the determination of compositions of the material. To determine the porosity of the biochar, BET analysis was used. To identify the functional groups in the biochar, a Fourier transform spectrophotometer model Agilent Technologies Cary 600 series was used. The calorific value for this investigation was measured using a calorimetric pump.

2.3 The preparation of synthetic waters

For the preparation of synthetic waters, the necessary amounts of nickel sulfate for each experiment were weighed on an analytical balance (Igi, 2017) and dissolved in water to obtain solutions with the stipulated concentrations, equivalent to 25 and 50 ppm.

2.4 Adsorption in packed bed with biochar

In a laboratory-scale adsorption column, 22 gr biochar was introduced as a packed bed, which produces a height of 20 cm in the column (Dalai et al., 2015a). Then, the nickel-contaminated solution was passed with an upflow of 2.5 L/h at a concentration of 50 mg/L and pH 8.5, and samples were collected at the outlet of the column every 15 min until reaching 120 min, to analyze the adsorption behavior. Once all the contaminated water had passed, the column was disassembled and the bed was changed, to start the next experiment with the new initial nickel concentration equivalent to 25 mg/L. After performing all experiments with different concentrations, the biochar was disassembled and the experiment was performed using the new height corresponding to 10 cm, which is equivalent to 11 gr of biochar (Dalai et al., 2015a) and the same procedure was performed as for a height of 20 cm.

2.5 Calculation of nickel removal percentages

To calculate the nickel removal percentages, the following equation was solved:

$$\%R = \frac{C_o - C_f}{C_o} \times 100\% \quad (1)$$

Where Co corresponds to the initial concentration and Cf to the final concentration. To know the final nickel concentration in each experiment, the water samples taken at the exit of the adsorption tower from time 0 to 120 minutes with intervals of 15 minutes were subjected to atomic absorption tests, in the contrAA® 800 D Spectrometer.

2.6 Construction of breakthrough curves and prediction of parameters for the design of adsorption columns

For the construction of the breakthrough curves, atomic absorption tests were carried out to determine the element nickel. The samples taken at the exit of the column from time 0 with intervals of 15 min up to 120 min, and in this way the nickel concentration at the exit of the tower at each time was obtained.
Subsequently, with these values, the graph of the relative concentrations, C/Co, versus the time at which the samples were taken was plotted, from which the breakthrough time, tb, was interpreted, which was taken at a relative concentration of 0.1 (McCabe et al., 2007).

3. Results and Discussion

3.1 Yield on biochar production

Biochar yield was higher as the particle size increased, establishing a direct relationship (Figure 1). The high percentage of the larger particles is due to the fact that as the particle size increases, the distance between the surface of the input biomass and its core increases, which retards the rapid flow of heat from the hot to the cold end. This temperature gradient favors biochar yield. In addition, by increasing the particle size, the steam formed during the thermal cracking of the biomass covers a greater distance through the carbon layer, causing more secondary reactions that result in the formation of more quantities of carbon (Tripathi et al., 2016). However, the yield of the biochar increased with the pyrolysis time of the rice husk because by increasing the residence time of the raw material, the repolymerization of the biomass constituents by giving them enough time to react is generated (Tripathi et al., 2016).

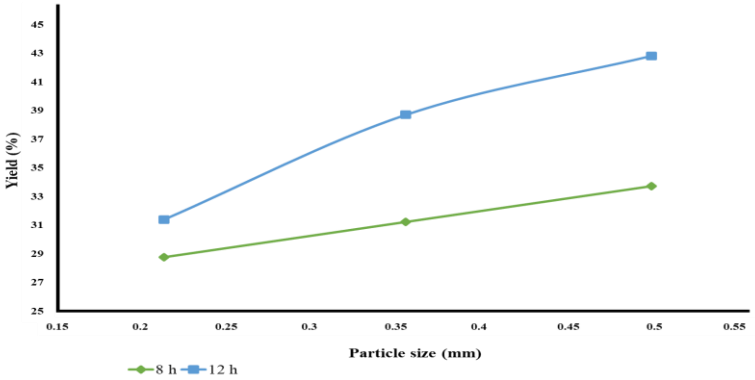

Figure 1: Yield on biochar production.

3.2 Carbon content

The percentage of carbon has no significant variation between different particle sizes and pyrolysis or residence times, i.e., neither the particle size of the biomass, nor the pyrolysis time of the biomass, affect the percentage of carbon present in the biochar, i.e., the carbon content of biochar can be varied by altering the feedstock and/or production conditions, where at high pyrolysis temperatures, woody and herbaceous biomass provides a more carbon-rich biochar compared to other feedstocks such as sludge and animal manures (Suliman et al., 2016). Now, although the main element of biochar is carbon, it also contains hydrogen, oxygen, ash, and trace amounts of nitrogen and sulphur.

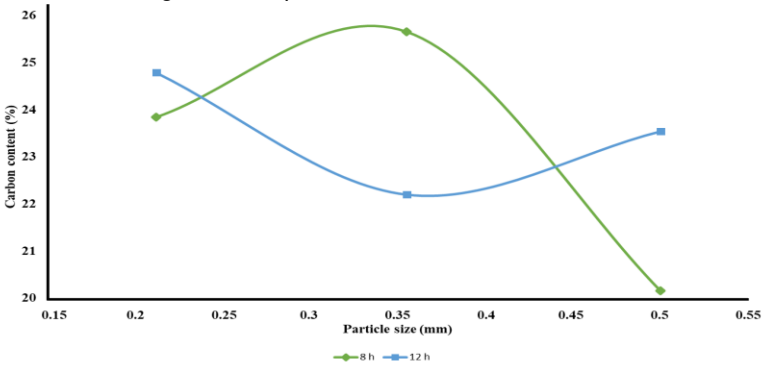

Figure 2: Carbon content of the biochar.

3.3 Surface area

The surface area of the biochar in both residence times presented a maximum growth in particle size of 0.355 mm, establishing that particle size as the optimum to obtain the largest amount of surface at the established pyrolysis conditions. This result is because huge particle sizes do not provide enough surface area, while in insignificant sizes, rupture or plugging can be generated in the pores (Fernandes et al., 2016). Additionally, there is an increase in surface area with increasing pyrolysis time.). Thus, the particle size and residence time showed favorable effects on the surface area of the biochar. Therefore, the highest surface area obtained in biochar at low pyrolysis temperatures is the biomass particle size of 0.355 mm and the pyrolysis time of 12 h.

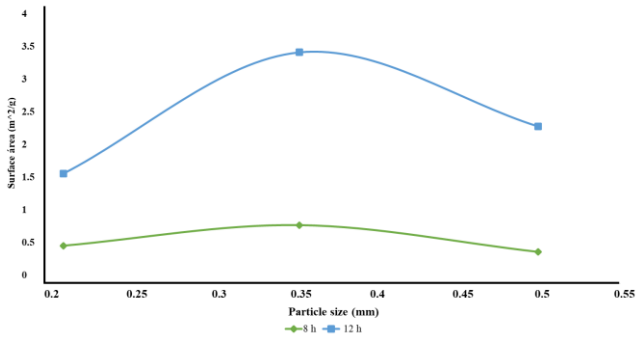

Figure 3: Surface area of the biochar.

3.4 Functional groups

The spectra in Figures A and B present band 1 with lengths of 2363.64 and 2360.44 cm-1 respectively, related to carbon dioxide present in the air (Mangrich, 2017), while for Figure C, in the little wide band 1 with a length of 2979 cm-1, the functional group alkanes are shown varying in a range from 2850 cm-1 to 3000 cm-1. Band 2 in Figures A and B of 1704.76 and 1701.87 cm-1, the presence of carboxylic acids is found, corresponding to the stretching of the carbonyl group (C=O). 2017). However, the soft band 3, in Figures A and B, with equal wavelengths of 1615.09 cm-1, indicates the functional group ketones with carbonyl group stretching (C=O) (Mandal et al., 2018). In Figure C, the soft band 3 at 1701.87 cm-1 represents the carboxylic acid functional group with the carbonyl group stretching (C=O), occurring later than for samples A and B.

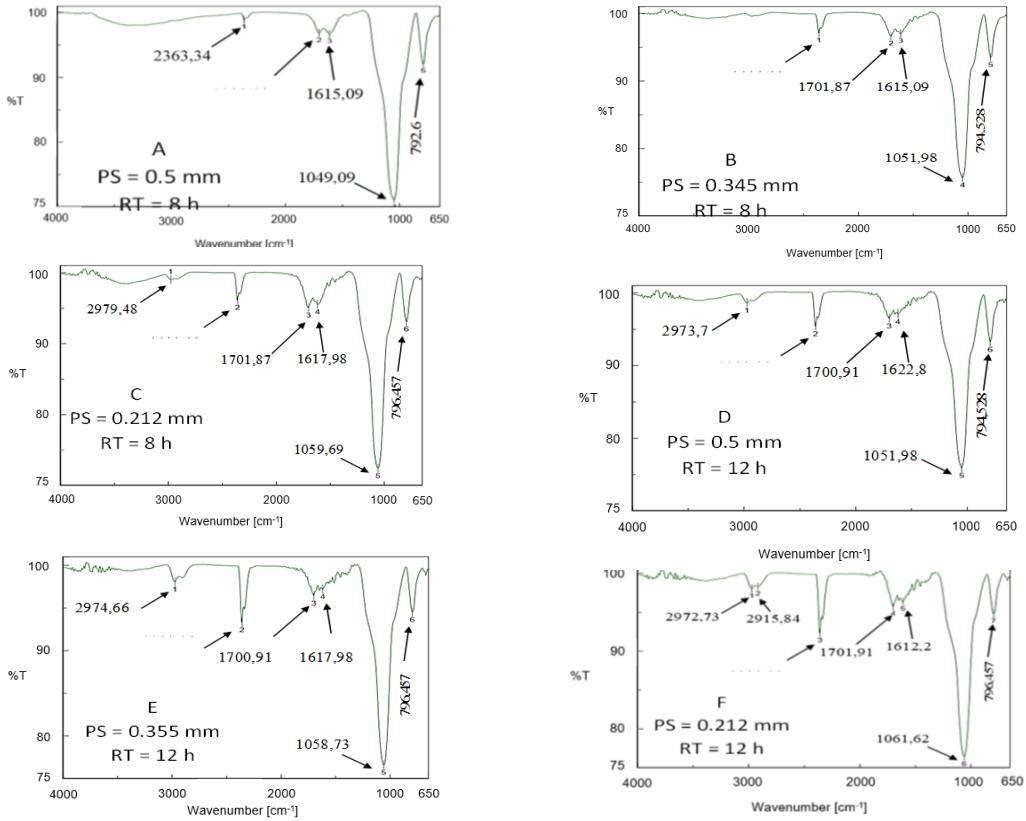

Figure 4: Functional groups of the biochar with the differents sizes.

The intense band 4 for Figures A and B, with lengths of 1049.09 and 1051.98 cm-1 respectively, represent the alcohol functional group, C-O single bonded alkoxy type, such stress band is presented in low wave number

because it is an alcohol without substituents. In Figures D, E and F, band 1 marked vibration 2973.7; 2974.6 and 2972.73 cm-1 respectively, representing the functional group alkanes ranging from 2850 cm-1 and to 3000 cm-1. They are used for burning; thus, they are used as fuels for energy supply (Zhang, et al., 2018). For band 3 in Figure D and E, the wavelength is equal with 1700.91 cm-1, showing carboxylic acids with the carbonyl group stretching (C=O) (Mangrich, 2017), but in band 3 in Figure F, it barely shows carbon dioxide with a band of 2360.44 cm-1. With respect to the infrared spectra of samples A, B, C, D, E, and F, it can be stated that the changes in the functional groups for the different particle sizes and pyrolysis times were not significant; however, in samples C and F, which have the smallest particle size (0.212 mm), the bands showed differences of one band with respect to the samples that were compared. The biochar studied present functional groups such as alkanes, carboxylic acids, alcohols, alkyl halides and ketones, which can form negative dipoles and attract the negative dipoles possessed by the functional groups of the contaminants.

3.5 Nickel removal

According to Figure 5, the percentage of removal is significantly dependent on the height of the bed and the initial concentration, including the interaction between these two, which is antagonistic because the height and the initial concentration have opposite effects on each other since we have obtained P-values lower than 0.05. Additionally, removal is favored in the experiment with greater height and lower concentration (20 cm and 25 ppm); contrary to what occurs when working with lower height and higher concentration (10 cm and 50 ppm).

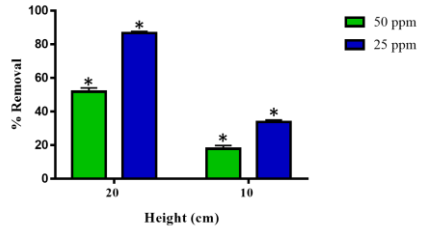

Figure 5: Percentage of Nickel Removal with the biochar.

3.6 Breakthrough curves and prediction of parameters for the design of adsorption columns

experiment (40 min). However, the stoichiometric capacity of the column was reached in a shorter time at higher concentration, therefore, the nickel concentration with which the water enters the bed has an inversely proportional relationship with the bed breakthrough time. However, the breakpoint and saturation point are reached in a shorter time if the bed height is decreased because the mass transfer occurs predominantly by the axial dispersion phenomenon, therefore, the nickel ions do not have enough time to diffuse throughout the mass of the adsorbent material (Taty-costodes, Fauduet, Porte, & Ho, 2005). Considering the above, the higher the bed height, the more time it takes for the bed to become saturated, which results in a longer lifetime and higher removal efficiency is reflected in the reduction of the area under the curve in experiments with higher bed height (Luo, Liu, Deng, & Lin, 2011). Figure 6 shows that the breakpoint was reached faster in the 50 ppm experiment (23.7 min) than in the 25 ppm

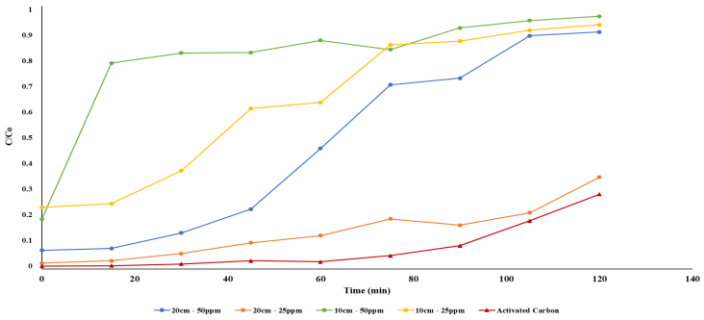

Figure 6: Breakthrough curves for process scaling.

4. Conclusions

The biochar yield is in accordance with those reported by other authors. Particle size and pyrolysis time showed favorable effects on biochar yield since biochar yield increases with larger biomass particle size (for the 0.5 mm case) due to structural characteristics and moderate pyrolysis times (for the 12 h case) due to changes in

chemical structure. However, biomass particle size and pyrolysis time have no influence on the percentage of carbon in the biochar, as it changes with the alteration of the feedstock and/or production conditions. As for the functional groups present in the biochar structure, they also coincided with those described in the literature, some were found such as alkanes, carboxylic acids, alcohols, alkyl halides and ketones, which give adsorbent characteristics to the material and ability to interact with different contaminants in aqueous media and soils, although the influence of pyrolysis time and particle size is significant. However, the surface areas of the biochar were low, so, in spite of having adequate carbon percentage and functional groups for adsorption, the formation of pores in the biochar for the conditions of temperature and residence time of the pyrolysis, was not benefited to obtain a large increase in the surface area, so, the adsorbate that can be removed with the area obtained for this biochar should be chosen, in addition to looking for alternatives for the activation of the carbon.

Finally, the adsorption process presents the highest removal percentages (86.03%) for heights of 20 cm biochar and initial concentration of 25 ppm nickel, so it has a potential applicability for processes that are developed with considerable bed heights and relatively small nickel concentrations. The breakthrough curves performed for each experiment show that with higher biochar heights and lower nickel concentrations the bed takes longer to reach its breakthrough point (46 min) and therefore to reach full saturation.

References

Abdelhadi, S. O., Dosoretz, C. G., Rytwo, G., & Gerchman, Y. (2017). Production of biochar from olive mill solid waste for heavy metal removal. *Bioresource Technology*, 244(August), 759–767. https://doi.org/10.1016/j.biortech.2017.08.013

Dalai, C., Jha, R., & Desai, V. R. (2015). Rice Husk and Sugarcane Baggase Based 74 Activated Carbon for Iron and Manganese Removal. *Aquatic Procedia*, 4, 1126– 1133. https://doi.org/10.1016/j.aqpro.2015.02.143

Dunnigan, L., Ashman, P. J., Zhang, X., & Wai, C. (2018). Production of biochar from rice husk : Particulate emissions from the combustion of raw pyrolysis volatiles. *Journal of Cleaner Production*, *172*, 1639–1645. http://doi.org/10.1016/j.jclepro.2016.11.107

Fernandes, I. J., Calheiro, D., Kieling, A. G., Moraes, C. A. M., Rocha, T. L. A. C., Brehm, F. A., & Modolo, R. C. E. (2016). Characterization of rice husk ash produced using different biomass combustion techniques for energy. *Fuel*, *165*, 351–359. http://doi.org/10.1016/j.fuel.2015.10.086

Igi, M. (2017). Utilization of fruit processing industry waste as green activated carbon for the treatment of heavy metals and chlorophenols contaminated water, 162, 958–972. https://doi.org/10.1016/j.jclepro.2017.06.083

Luo, X., Liu, F., Deng, Z., & Lin, X. (2011). Removal of copper (II) from aqueous 77 solution in fixed-bed column by carboxylic acid functionalized deacetylated konjac glucomannan. *Carbohydrate Polymers*, 86(2), 753–759. https://doi.org/10.1016/j.carbpol.2011.05.020

Mangrich, A. S. (2017). Evaluation of waste biomasses and their biochars for removal of polycyclic aromatic hydrocarbons. *Aquatic Procedia, 200*, 186–195. http://doi.org/10.1016/j.jenvman.2017.05.084

McCabe, W., Smith, J., & Harriott, P. (2007). Operaciones unitarias en ingeniería química (7ma ed.). Ciudad de México.

Noë, J. Le, Billen, G., & Garnier, J. (2017). How the structure of agro-food systems shapes nitrogen , phosphorus , and carbon fl uxes : The generalized representation of agro-food system applied at the regional scale in France. *Science of the Total Environment*, *586*, 42–55. http://doi.org/10.1016/j.scitotenv.2017.02.040

Popa, N., & Visa, M. (2017). The synthesis , activation and characterization of charcoal powder for the removal of methylene blue and cadmium from wastewater. *Advanced Powder Technology*, 28(8), 1866–1876. https://doi.org/10.1016/j.apt.2017.04.014

Sajid, M. (2017). Removal of heavy metals and organic pollutants from water using 79 dendritic polymers based adsorbents : A critical review. *Separation and Purification Technology*. https://doi.org/10.1016/j.seppur.2017.09.011

Singh, U. K., & Kumar, B. (2017). Pathways of heavy metals contamination and associated human health risk in Ajay River basin, India. *Chemosphere*, 174, 183–199. https://doi.org/10.1016/j.chemosphere.2017.01.103

Suliman, W., Harsh, J. B., Abu-lail, N. I., Fortuna, A., Dallmeyer, I., & Garcia-perez, M. (2016). Modification of biochar surface by air oxidation : Role of pyrolysis temperature. *Biomass and Bioenergy*, *85*, 1–11. http://doi.org/10.1016/j.biombioe.2015.11.030

Taty-costodes, V. C., Fauduet, H., Porte, C., & Ho, Y. (2005). Removal of lead (II) 80 ions from synthetic and real effluents using immobilized Pinus sylvestris sawdust : Adsorption on a fixed-bed column, 123, 135–144. https://doi.org/10.1016/j.jhazmat.2005.03.032

Tripathi, M., Sahu, J. N., & Ganesan, P. (2016). Effect of process parameters on production of biochar from biomass waste through pyrolysis: A review. *Renewable and Sustainable Energy Reviews*, *55*, 467–481. http://doi.org/10.1016/j.rser.2015.10.122

Tsai, W. T., Lee, M. K., & Chang, Y. M. (2007). Fast pyrolysis of rice husk : Product yields and compositions. *Bioresource Technology, 98*, 22–28. http://doi.org/10.1016/j.biortech.2005.12.005

Zhang, S., Zhu, S., Zhang, H., Chen, T., & Xiong, Y. (2018). Pyrolysis Catalytic fast pyrolysis of rice husk : E ff ect of coupling leaching with torrefaction pretreatment. *Journal of Analytical and Applied Pyrolysis*, *133*(April), 91–96. http://doi.org/10.1016/j.jaap.2018.04.016